PAPER

New proton conducting membranes with high retention of protic ionic liquids†

Yun Sheng Ye,[a] Ming Yao Cheng,[b] Ji Yong Tseng,[a] Gao-Wei Liang,[a] John Rick,[a] Yao Jheng Huang,[c] Feng Chih Chang[c] and Bing Joe Hwang*[a]

New proton conducting membranes, exhibiting a high proton conductivity (10^{-2} S cm^{-1}, without humidification at 160 °C), based on the ionic liquid (IL) 1-butyl-3-methylimidazolium tetrafluoroborate (BMIm-BF$_4$) were investigated. The incorporation of a similar initial IL loading was found to reduce the proton conductivity loss of a sulfonated polydiacetylene based membrane, *i.e.* SPDA70-IL70 by 19.2% and IL-based Nafion by 64.6%; additionally, the SPDA70-IL70 was able to maintain a proton conductivity of more than 10^{-3} S cm^{-1} after centrifugation. The introduction of both a cross-linked structure and a high degree of sulfonation into the polymer matrix, resulted in significant improvements to the membranes' thermal properties, the dispersion of ionic domains, and the retention of IL—together with a reduction of proton conductivity loss. The membranes, which have a high degree of sulfonation with thermally cross-linkable diacetylene in the polymer's main chain, avoid the drawback of poor miscibility commonly associated with sulfonated polymers and cross-linking agents. When the composite membrane was used in a H$_2$/O$_2$ fuel cell without humidification at 100 °C, a power density > 250 mA cm^{-2} was achieved together with a maximum current denisty of 122 mW cm^{-2}.

Introduction

Ionic liquids (ILs) are composed of organic cations (*e.g.*, imidazolium, pyridinium, or tetraalkylammonium) and anions (halide, tetrafluoroborate, hexafluorophosphate, triflate, amidotriflate, *etc*); they have highly variable aqueous solubilities (depending upon the anion), ranging from highly soluble to immiscible. ILs are attracting significant attention, in many fields of chemistry and industry, because of their unique physicochemical properties, such as their high ionic conductivity, high polarity, high density, high heat capacity, and high thermal and chemical stability.[1–5] These characteristic features of ILs offer suitable properties for polymer electrolyte membranes (PEMs) and have been extensively studied to replace liquid electrolytes, which are toxic, flammable and able to leach out.[6–8]

For polymer electrolyte membrane fuel cells (PEMFCs), the PEM is one of the key issues because it acts as an electrolyte to transport protons from the anode to the cathode. One of the main challenges in the development of PEMFCs is to develop membrane materials with high operating temperatures (above 100 °C), to achieve higher reaction kinetics at both electrodes,

less poisoning at the anode, and easy heat and water managements of the stacks.[9–13] For water-swelled polymeric systems, however, the conductivity is strongly humidity dependent, so they cannot be used above 100 °C due to the loss/evaporation of water, which results in a significant loss of conductivity.[14] In contrast to which ILs are suitable for high temperature applications, because they can act as proton transferring carriers in anhydrous conditions, while exhibiting: excellent chemical and thermal stabilities, non-flammability and non-volatility. Therefore, many studies have been carried out to develop IL-based membranes with high proton conductivities that can operate at higher temperatures (100–200 °C) in anhydrous conditions.[15–29] The development of IL-based PEMs mainly focuses on mixtures of well-known polymers with IL using various strategies, such as: the *in situ* polymerization of vinyl monomers in ILs,[18–20] doping polymers with ILs,[21–23] and solution casting IL-polymer solutions.[24–29]

Although the IL-based membranes allow PEMFCs to operate at higher temperatures in anhydrous conditions while avoiding water dependent conductivity, they have a major drawback, *i.e.* the progressive release of ILs leading to a long-term decline in the performance of the fuel cells.[30,31] To solve the leaching problem, approaches incorporating inorganic fillers[32,33] into the polymer membranes and the formation of cross-linkable structures appear to be efficient approaches towards retarding the degree of methanol diffusion and water uptake, while enhancing the polymer's mechanical properties and dimensional stability.[34–38] More recently, Yan and Lu *et al.*[20] reported protic IL-based hybrid proton conducting membranes, wherein the addition of silica

[a]Department of Chemical Engineering, National Taiwan University of Science and Technology, Taipei, Taiwan. E-mail: bjh@mail.ntust.edu.tw
[b]Graduate Institute of Engineering, National Taiwan University of Science and Technology, Taipei, Taiwan
[c]Institute of Applied Chemistry, National Chiao-Tung University, Hsin-Chu, Taiwan
† Electronic supplementary information (ESI) available. See DOI: 10.1039/c0jm02878a

This journal is © The Royal Society of Chemistry 2011

J. Mater. Chem., 2011, **21**, 2723–2732 | 2723

fillers into the composite membranes was shown to both enhance the conductivity and prevent the release of the IL component from the composite membranes. To the best of our knowledge, the incorporation of cross-linking structures in the PEMs will enhance the retention of IL in the membrane; however, the presence of the cross-linking structure appears to lower proton conductivity. Thus, the development of more efficient membranes with both improved proton conductivities and enhanced retention of IL in the membrane remains an important challenge.

In the present study, we describe the synthesis and characterization of IL-based cross-linked membranes. The thermal cross-linkable diacetylene-containing polymer, sulfonated polydiacetylene (SPDA), was synthesized and used as the polymer matrix because the diacetylene groups have the ability to cross-link under irradiation or with heat treatment without the evolution of volatile byproducts.[39,40] In addition, such main chain type cross-linked polymers avoid the drawback of poor miscibility often associated with common sulfonated polymer and cross-linking agents. Polymers with various degrees of sulfonation (DS) of SPDA were synthesized via oxidative coupling polymerization and were blended with 1-butyl-3-methylimidazolium tetrafluoroborate (BMIm-BF$_4$) to form IL-based membranes (SPDA-IL) after a thermal cross-linking process. The influences of the DS and the network structure on the properties of the resulting composite membrane were systematically investigated with respect to: the IL uptake, the leaching of IL by centrifugation, morphology, ionic conductivity and thermal stability. In addition, the influence of IL retention properties on proton conductivity, based on SPDA and recast Nafion containing IL, has also been compared in this study.

Experimental section

Materials

Nafion (5%) dissolved in a solvent comprising water and methanol, Bisphenol A (≥99%), 2,5-dihydroxybenzenesulfonate, tetra-n-butylammonium bromide (≥98.0%), sodium tetra-fluoroborate (≥98.0%), N,N,N′,N′-tetramethylethylenediamine (TMEDA) (≥99%), copper-iodine (CuI) (≥99.5%), pyridine (≥99%), hydrochloride acid (36.5–38.0%), dimethylformamide (DMF) (≥99%), acetonitrile (HPLC grade), acetone (≥99.9%), ethanol (EtOH) (≥99.5%) and dimethyl sulfoxide (DMSO) (≥99.9%) were purchased from Sigma-Aldrich and used as received. 1-Bromobutane (≥99%), 1-methylimidazole (≥99%), propargyl bromide (80 wt. % in toluene) and potassium carbonate (≥99.0%) were purchased from Acros and used as received. 4,4′-(Propane-2,2-diyl)bis[(prop-2-ynyloxy)benzene] (PBPB), potassium 2,5-bis(prop-2-ynyloxy)benzenesulfonate (PBPBS) and the ionic liquid [1-butyl-3-methylimidazolium tetrafluoroborate (BMIm-BF$_4$)] were synthesized according to a modified procedure described elsewhere.[41,42] (See the ESI†).

Sulfonated polydiacetylene (SPDA)

To a dried three-neck, round-bottomed flask were added: CuI (11.5 mg, 0.11 mmol), N,N,N′,N′-tetramethylethylenediamine (TMEDA) (14 mg, 0.12 mmol), pyridine (0.185 g, 2.35 mmol), and 5 mL of anhydrous dimethyl sulfoxide (DMSO). To the flask

was attached a water condenser and an inlet and outlet for oxygen. The reaction mixture was warmed to 50 °C while oxygen was bubbled through. After 1 h, different ratios of the monomers PBPB and PBPBS (15 wt% solid content) in 10 mL of DMSO were added to the catalyst mixture to generate different polymers (Table 1). After 24 h, 8 mL of DMSO was added to the viscous solution, and the polymer was precipitated in 400 mL of methanol containing 2% HCl. The gray fibrous polymer was filtered and immersed in 50 mL of methanol containing 5% HCl with stirring over night. The solid was filtered and washed with methanol–water several times and dried under vacuum at 60 °C (yield 73%) (Scheme 1).

^{1}H NMR (d$_6$-DMSO): δ 1.58 (g), 4.91 (a), 6.86 (e), 6.95 (c), 7.00 (d), 7.13 (f), 7.32 ppm (b) (Fig. 1).; ^{13}C NMR: δ 31.33 (19), 41.99 (18), 56.37–58.35 (3, 10, 13), 70.76 (1, 11), 77.04 (2, 12), 114.74 (15), 116.23–117.63 (5, 6, 8), 128.30 (16), 138.38 (7), 144.08 (17), 148.96 (9), 151.61 (4), 155.33 ppm (14) (Fig. 2).

Membrane preparation

SPDA and the BMIm-BF$_4$ (cf. Table 1) were dissolved in DMSO at room temperature, to give a 15 wt% solution which was stirred overnight. The resulting solution was cast onto a glass plate and heated at 60 °C for 24 h to slowly evaporate the solvent and then heated at 180 °C for 4 h. The resulting membranes were blotted with kimwipes to remove surplus IL. The Nafion-IL membrane was prepared by a solution casting method described elsewhere.[26]

Monomer and polymer characterization

^{1}H NMR and ^{13}C NMR spectra were recorded at 25 °C using an INOVA 500 MHz NMR spectrometer. Solid state ^{13}C NMR spectra were recorded on a Buuker-400 MHz instrument using tetramethylsilane as an internal reference. FTIR spectra were obtained with a Nicolet Avatar 320 FTIR spectrometer; 32 scans were collected at a spectral resolution of 1 cm^{-1}. The ion exchange capacities (IECs) were determined by titration as in our previous study.[38,39] Wide-angle X-ray diffraction (WAXD) spectra were recorded for powdered samples using a Rigaku D/max-2500 type X-ray diffraction instrument. SAXS experiments were performed using the BL23A SWAXS instrument at the National Synchrotron Radiation Research Center (NSRRC), Taiwan, using a 10 keV (wavelength λ = 1.24 Å) beam with a 0.5 nm diameter. The scattering wavevector transfer q = $4\pi\lambda^{-1}\sin\theta$ is defined by λ and the scattering angle 2θ of X-rays. Samples for SAXS (thickness = 150∼200 μm) were sealed between two thin Kapton windows (80 μm thickness each) and measured at an ambient temperature ∼26 °C. The proton conductivity of the membrane was determined with an ac electrochemical impedance analyzer (PGSTAT 30), and the experiments involved scanning the ac frequency from 100 kHz to 10 Hz at a voltage amplitude of 10 mV. A DuPont Q100 thermo-gravimetric analyzer (TGA) was utilized to investigate the thermal stability of the membranes; the samples (∼10 mg) were heated from ambient temperature to 850 °C under a nitrogen atmosphere at a heating rate of 20 °C min^{-1}. The stability of the membranes was tested by measuring their proton conductivities at 160 °C, after thermal treatment at the same temperature for a designated time. The centrifugal test was carried out using a centrifugal process as detailed in our previous

Table 1 Characterization of sulfonated polydiacetylene membrane and composite membrane

Polymer	Theoretical content of PBPBS (mol%)[a]	Measured content of PBPBS (mol%)[b]	Theoretical IEC (meq g^{-1})[b]	Measured IEC (meq g^{-1})[c]	Reaction temp. (°C)[d]
SPDA50	50	49.5	1.68	1.57	200.9
SPDA60	60	58.8	2.04	1.99	187.9
SPDA70	70	68.0	2.41	2.32	175.9
PDA	0	0	0	0	209.4

[a] Determined from the initial feed ratio of PBPBS. [b] Calculated from ^{1}H NMR spectra. [c] IEC measured with titration. [d] Reaction exotherm temperature obtained from DSC at a heating rate of 20 °C.
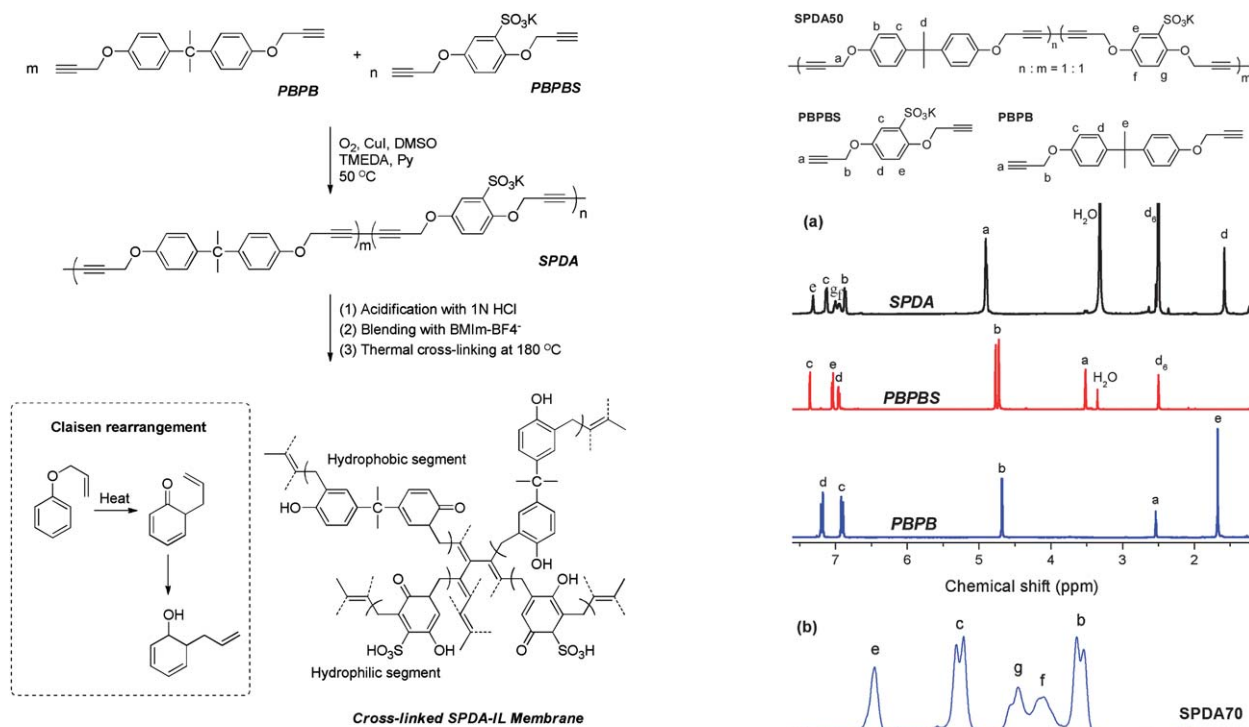
Scheme 1 Schematic representation of the preparation of the cross-linked SPDA-IL membrane.

study.[43] The IL-based membrane was poured into centrifugal filters (MICORSEP 30 K OMEGA, PALL). The centrifugal process was performed at 20000 rcf (relative centrifugal force) and 25 °C for several cycles until no weight loss was observed in the membrane. The proton conductivity of these membranes was measured at 160 °C. The electrode system, electrochemical procedure, fabrication of membrane electrode assembly (MEA), and the single-cell test procedure are described in the ESI†.

Results and discussion

Monomer and polymer synthesis

Monomers PBPB and PBPBS were prepared with high yields from propargyl bromide. The ^{1}H-NMR (d$_6$-DMSO, 25 °C) spectra of the monomers are shown in Fig. 1a, wherein the presence of propargyl protons, at 2.54 and 3.53 ppm respectively, for the monomers PBPB and PBPBS is apparent. The corresponding ^{13}C NMR (d$_6$-DMSO, 25 °C) shows resonances at 78.28 and 79.76 ppm, indicating the propargyl structure. The
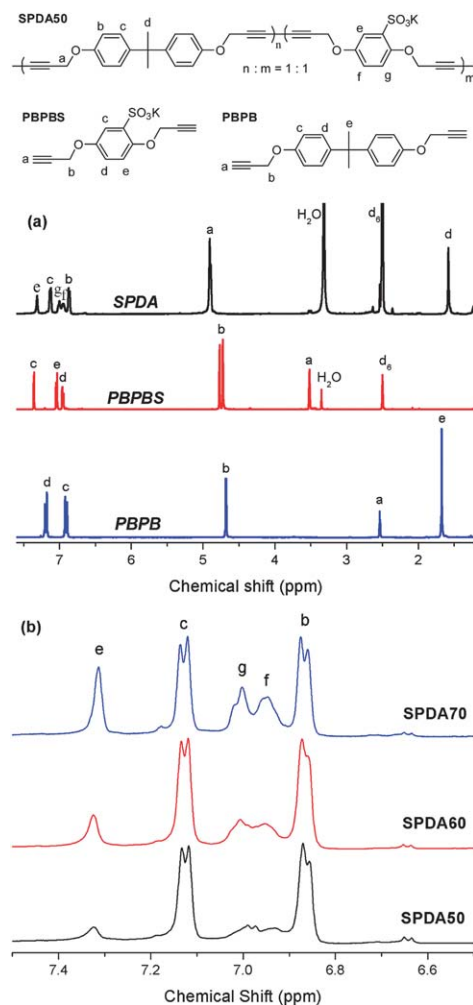

Fig. 1 (a) ^{1}H-NMR (d$_6$-DMSO, 25 °C) spectrum of PBPB, PBPBS and SPDA50. (b) ^{1}H-NMR (d$_6$-DMSO, 25 °C) spectrum of SPDA50-70.

FTIR spectrum is in agreement with the structure of the monomer PBPBS as indicated by the presence of bands at 3286 and 1181 cm^{-1}, corresponding to propargyl and sulfonic acid structures, respectively.

The synthesis of the three sulfonated polydiacetylenes (SPDA) SPDA50, 60 and 70, was carried out using the oxidative coupling method developed by Hay (Scheme 1).[44] SPDA50-70 were obtained using three different PBPB to PBPBS ratios. The degree of sulfonation (DS) in the final copolymers was determined by ^{1}H NMR (d$_6$-DMSO, 25 °C) from the integration of aromatic
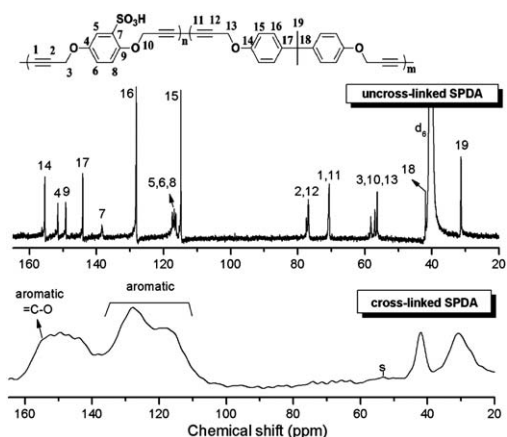
Fig. 2 ^{13}C-NMR spectrum of non-crosslinked and crosslinked SPDA50.

groups of the monomers PBPB [marked as 'f' and 'e' in the molecular formula in Fig. 1b] and PBPBS, [marked as 'b', 'c', and 'd' in the molecular formula in Fig. 1b]. Table 1 shows that the PBPB to PBPBS ratios in the final polymers were found to be very close to those in the feed ratios, allowing them to be easily adjusted and controlled. Moreover, a similar result was also observed for the measured ion exchange capacity (IEC) values for SPDA membranes, which were close to the theoretical values. The ^{1}H NMR and ^{13}C NMR spectra of the polymers were consistent with their assigned structures. No residual ethynyl protons (–C≡CH), due to unreacted acetylene groups (–C≡C–), were observed for the polymers by ^{1}H NMR (Fig. 1a and 1b). The ^{13}C NMR spectra also showed that the terminal ethynyl carbons were transformed into diacetylenic carbons after polymerization. For example, the two diacetylenic carbons at 70.59 and 77.04 ppm in the spectrum of SPDA50 (Fig. 2) replace the two ethynyl carbons at 78.28 and 79.76 ppm in the spectra of the monomers PBPB and PBPBS respectively. These results indicate that the different DS of SPDA were successfully synthesized by oxidative coupling.

Cross-linking behavior of polymer with ionic liquid

The cross-linking of SPDA50–70 and PDA (polydiacetylene) was examined by DSC as shown in Fig. 3a. Pure PDA exhibits a single sharp peak at 209.9 °C, which is attributed to the cross-polymerization of diacetylene. It has been reported that the cross-polymerization of diacetylene often takes place in this temperature range for aliphatic diacetylenes.[45–47] Fig. 3a shows that the SPDA membranes (SPDA50–70) display an exotherm that began around 130.8 °C, peaked above 175.9 °C, and extended to 318.4 °C. The nature of such a dramatic difference may be due to structural rearrangements facilitated by the higher DS of aromatic diacetylenes during cross-linked polymerization. In addition, for SPDA membranes, the exotherm peak temperature decreased with an increase in the DS of the membrane. These observations simply reflected the increase in the local concentration of sulfonated segments with reactive diacetylene groups facilitating the ease of thermal activation.[48,49] The SPDA50 was taken as an example to study the curing behavior by DSC after thermal treatment (at 180 °C) with designed times (30–240 min). As shown in Fig. 3b, the exotherm decreased
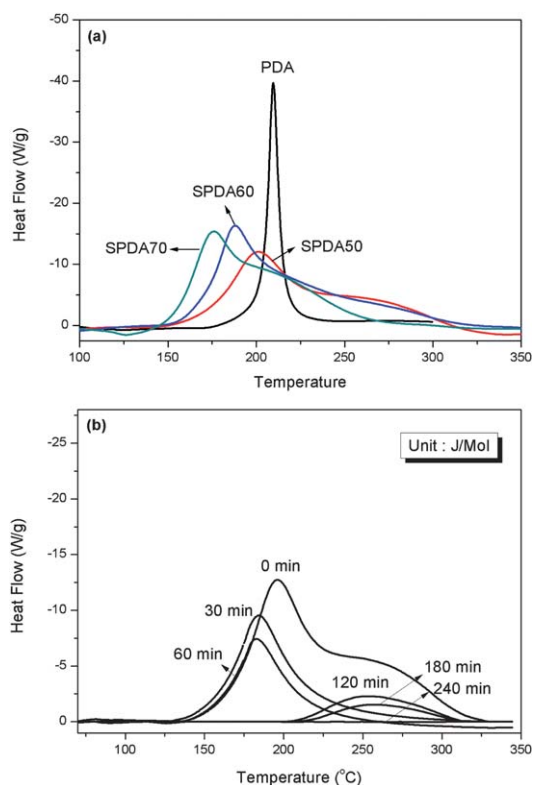

Fig. 3 (a) DSC curves of non-crosslinked membranes (PDA and SPDA50–70). (b) DSC curves of uncross-linked SPDA50 after thermal treatments (at 180 °C) with designated time (30–240 min).

gradually and disappeared completely after 240 min. These results indicate the complete cross-polymerization of the diacetylene in the SPDA membrane after 240 min at 180 °C.

The cross-linking of the membrane after the incorporation of IL into the polymer matrix was examined by FTIR. Fig. 4 shows the FTIR spectra of the non-crosslinked SPDA50, crosslinked SPDA50, SPDA50-IL composite membrane, and pure BMIm-BF[4]. SPDA50 was selected as a typical example to analyze the cross-linking behavior of IL-based membranes. The spectrum of pure BMIm-BF[4] shows various characteristic peaks associated with the IL structure. The first two bands at 3166 and 2943 cm^{−1}
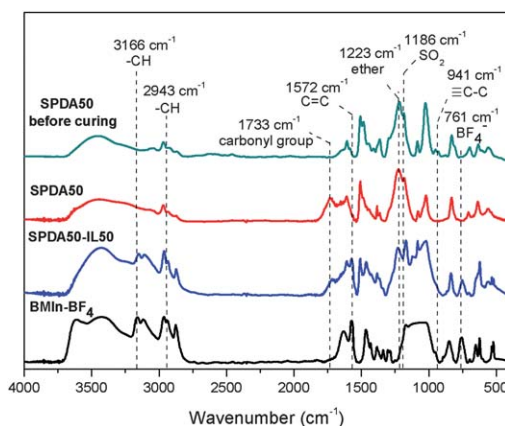

Fig. 4 FTIR spectrum of non-crosslinked SPDA50, crosslinked SPDA50, SPDA50-IL composite membrane, and pure Bmin-BF[4].

represent the –CH groups of the imidazole ring of the Bmin-BF$_4$, where the signal for the C=C double bonds of the imidazole ring is around 1572 cm^{-1}. The bands at 1121 and 754 cm^{-1} correspond to strength vibrations of the B–F bonds in BF$_4^-$, relating to the structure of the anion.[50,51] The spectrum of SPDA50 before curing was characterized by the symmetric stretching vibration of the C–O–C groups at 1223 cm^{-1}, the ≡C–C stretching vibration band at 912–970 cm^{-1}, and the symmetric stretching vibration of the sulfonic acid groups around 1186 cm^{-1}. After cross-linking, the intensity of the ≡C–C stretching vibration band at 912–970 cm^{-1} decreased, while a new peak appeared at 1733 cm^{-1} (due to carbonyl groups). These results suggest that the –CH$_2$O– linkage is involved in the thermal-curing process to a certain extent and is responsible for the formation of the new carbonyl in the cross-linking process. These results are similar to the previous results for thermal cross-linked polydiacetylene,[46] indicating that a Claisen rearrangement reaction has taken place during the thermal cross-linking process (Scheme 1).[52,53] The ^{13}C NMR spectrum of SPDA50 (Fig. 2) also confirmed extensive reactions involving the diacetylene and methyleneoxy groups, as the peaks at 70.59 and 77.04 ppm (alkyne carbons) and at 56.37–58.27 ppm (–CH$_2$O–) almost completely disappeared. Similar results also showed in other SPDA-IL membranes which indicate that the diacetylene groups were completely reacted, incorporating IL into the polymer matrix. Fig. 5 shows a photograph of the resulting SPDA-IL membrane (SPDA70-IL70 with the thickness of 160 μm). These membranes are flexible and can be cut into any desired sizes and shapes, whereas the pure form polymeric matrix (SPDA) (without ILs) is stiff and brittle.

Ionic liquid uptake and centrifugal test

The ionic liquid used in the present study was 1-butyl-3-methylimidazolium tetrafluoroborate (BMIm-BF$_4$). This IL has been reported to a have dynamic viscosity of 2.33 P at 30 °C and a conductivity of 0.86 mS cm^{-1} at 60 °C.[54] The loss after centrifugation and thermal decomposition temperatures of SPDA membranes with different ratios of IL loading are shown in Table 2. The amount of absorbed IL into the membranes impregnated after the cross-linking procedure is less than the theoretical content of IL. In comparison with the Nafion-IL membrane, the difference between the theoretical and the measured content of IL in SPDA is similar. The lower IL uptake for the measured value can be mainly attributed to the presence of cross-linking in the polymer chains that restricts IL swelling in
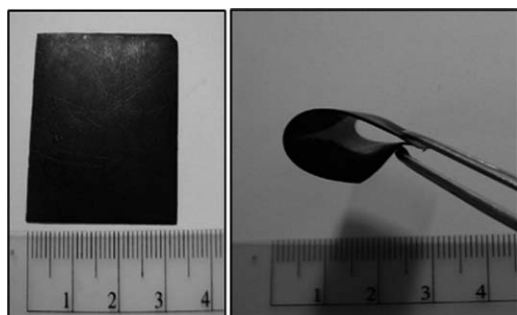

Fig. 5 A photograph of the SPDA-IL membrane (SPDA70-IL70).

Table 2 Quantity of ionic liquid uptake, IL loss after centrifugal test and thermal decomposition temperature of membranes

Membrane	Theoretical IL uptake (wt%)^a	Measured IL uptake (wt%)^b	Loss after centrifugal test (wt%)	Remaining IL in membrane (wt%)	$T_{d5}{}^c$	$T_{d10}{}^c$
SPDA50-IL50	50	28.6	1.6	27.4	311.1	340.1
SPDA50-IL60	60	34.0	4.5	30.9	312.6	349.4
SPDA50-IL70	70	40.4	11.5	32.7	316.6	348.4
SPDA60-IL70	70	43.8	11.3	36.6	319.4	348.9
SPDA70-IL70	70	47.5	10.5	41.3	317.2	349.1
Nafion-IL50	50	47.8	22.0	33.1	359.6	382.8

^{a} Determined from the initial IL loading in the polymer. ^{b} Calculated from TGA, using pristine polymer compared with composite membrane. ^{c} Decomposition temperature as calculated at 5% and 10% weight loss in N$_2$, as assessed by TGA at a heating rate of 20 °C min^{-1}.

This journal is © The Royal Society of Chemistry 2011

J. Mater. Chem., 2011, **21**, 2723–2732 | 2727

the membrane. Generally, the absorption of IL in the membrane is dependent on the availability and accessibility of ionic groups. As the membrane content of sulfonic acid groups increases, more become accessible and available for ion exchange with the cation of the IL. Therefore, the content of IL in the SPDA membrane is expected to increase with increasing DS. A decrease in the membrane weight was observed after the leaching test. Choudhury et al.[22] demonstrated that the IL molecules in the membrane can be classified into two parts: (a) where the IL is physically residing within the membrane and is not bound through interaction, and (b) where the IL interacts with the membrane through electrostatic interactions. In this study, the centrifuge was used to probe the IL holding levels by physical separation of the solid (polymer) and the liquid phase (IL). The centrifugal test was carried out to determine the amount of IL that may be lost from the membrane. This test does not reflect real operating conditions for the membranes, but it helps to evaluate the long-term stability of these composite membranes. The percentage losses (%) and residual weights (wt %) of IL are shown in Table 2. All samples were subjected to a rotation speed of 20 000 rpm in the centrifugal test. Fig. 6 shows the amount of IL lost from the sample SPDA70-IL70 as a function of rpm. It was evident that a centrifuge rotation speed of 20 000 rpm could easily differentiate between strongly interacting IL and weakly interacting IL. The amount of IL lost from the SPDA membranes (all with DS = 50), was compared to the amount of IL initially loaded. The results indicated that a fraction of the IL was physically residing within the membrane and not bound through interactions, and was hence lost during centrifugation. The retaining capability within the polymer for the IL was improved by increasing the DS of SPDA membrane, indicating that to a significant degree ILs interact with the membrane through electrostatic interactions (Scheme 2). To clarify the effects of cross-linking on the retention of the IL, SPDA membranes (SPDA50-IL70) with various degrees of cross-linking (49.5–100%) were investigated (ESI†). It is not surprising that the IL loss after the centrifugation test decreased as the degree of membrane cross-linking increased, due to the presence of more cross-linked structure able to prevent the release of IL. The retention of IL, from SPDA50-IL70, was compared to that of SPDA70-IL70 and Nafion-IL50, since
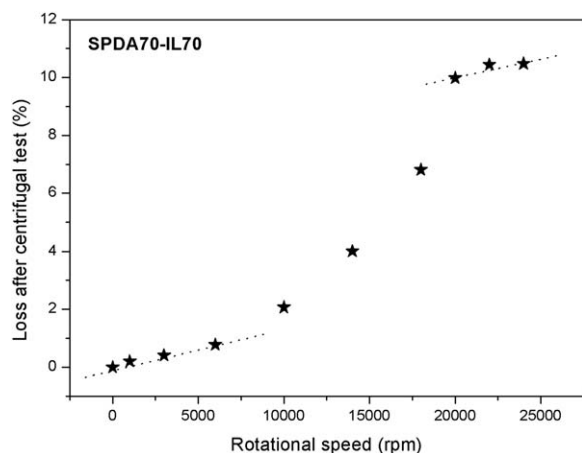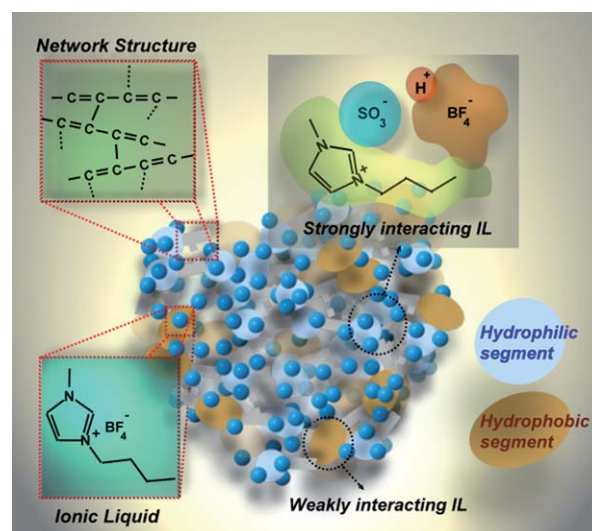

Scheme 2 Graphical representation of a crosslinked SPDA-IL membrane.

similar IL loadings are found in these membranes. Higher amounts of IL were lost during centrifugation from the Nafion-IL50 membrane (22.0%) than the SPDA70-IL70 membrane (10.5%), indicating a higher number of sulfonic acid groups (IEC = 2.32 meq g^{-1}) to be present in the SPDA70-IL70 membrane. In addition, the network structure throughout the membrane allows for the entrapment of more IL in the membrane and prevents the release of IL component from the composite membranes.

Morphological changes in the presence of ionic liquid

In order to understand and explain the ionic conductivity results obtained from the cross-linked SPDA containing hydrophilic IL (BMIm-BF$_4$), the morphology of the membranes was studied by X-ray diffraction (XRD) and small-angle X-ray scattering (SAXS). In general, the cluster network model [55,56] and the core shell model[57,58] are the two main models most widely used to explain the morphologies and ionic conductivities of water swollen Nafion membranes. These models feature a spherical ionic cluster phase within a continuous matrix phase. On the basis of quantitative analysis of published SAXS data, it has been shown that the angular position of the ionomer peak in the SAXS profile represents the average spacing between centers of ionic clusters. Recently, the morphology of proton conductivity membranes containing ILs has been investigated by small-angle X-ray scattering (SAXS).[17,26,59] Swelling of the membrane ionic domains was expected to cause changes in the ionomer's morphology, especially in the ionomer peak of the SAXS profile. SAXS scattering profiles, plotted as an intensity vs. scattering vector q on a log–log plot, at various IL swelling levels and DS of the cross-linked SPDA are shown in Fig. 7a. The "ionomer peak" is presented in SPDA50-IL50 membrane at q = 0.077 A^{-1} (d = 81.6 Å) and q = 0.107 A^{-1} (d = 58.7 Å). The presence of a weak ionomer peak at q = 0.107 A^{-1} (d = 58.7 Å) may result from the restriction of the ionic domains by the cross-linked structure, leading to the small size of ionic domains containing IL. The membrane used in the present study was a cross-linked polymer
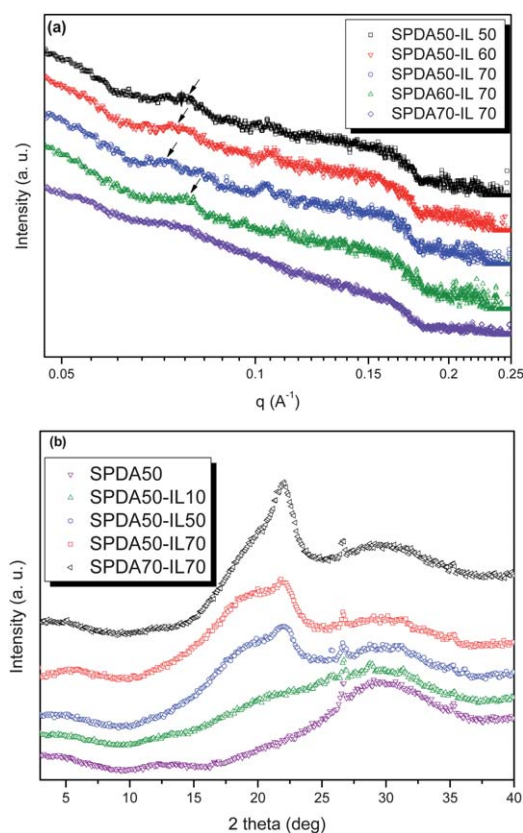

Fig. 6 Amount of IL lost from sample SPDA70-IL70 as a function of rpm.

Fig. 7 (a) SAXS spectra of SPDA50-IL50, SPDA50-IL60, SPDA50-IL70, SPDA60-IL70 and SPDA70-IL70. (b) XRD spectra of SPDA50, SPDA50-IL10, SPDA50-IL50, SPDA50-IL70 and SPDA70-IL70.

and such cross-linked structures generally form small ionic domains.[34–38] The ionomer peak systematically shifted to a lower q as the IL content increased, i.e., 0.077 A^{-1} and 0.107 A^{-1} at 50 wt % to 0.072 A^{-1} and 0.103 A^{-1} at 70 wt % BMIm-BF$_4$, respectively. This increase in inter-cluster spacing may correspond to an increase in cluster size through plasticization with IL. An increase in d spacing is generally observed for many ionomers in the literature.[17,26,59] In case of the membrane containing the same IL loading, the ionomer peak slightly decreases with an increase in the DS of the SPDA matrix (Table 2), which is related to the presence of the higher content of sulfonic acid groups in the membrane. Moreover, the ionomer peak at q = 0.103 A^{-1} (d = 61.0 Å) disappeared with higher DS (DS = 70). Although the clustering of IL occurs due to aggregation in the hydrophobic cross-linked structure, as more sulfonic acid groups in the membrane can favor the accessibility of hydrophilic IL to ion exchange with sulfonic acid groups of the membrane. Therefore, a higher degree of DS in the polymer matrix allows more IL to ion exchange with sulfonic acid groups and results in homogeneous distribution of IL in the membrane matrix.

The morphological change in the presence of IL was also checked by XRD, as shown in Fig. 7b. For a pure SPDA membrane, the boarder amorphous peak appeared at a value of 2θ = 30.06° (d = 2.97 Å). Upon incorporating 10 wt% of BMIm-BF$_4$, a new boarder shoulder appeared at 2θ = 21.04° (d = 4.22 Å), an increased trend was observed with an increase in the IL loading in the membrane, suggesting that the polymer matrix was

compressed in the membrane due to the distribution of IL along the polymer chains, or that the polymer chains were restricted by IL domains to produce the different formation of cross-linked structure.

Ionic conductivity and single-cell test of composite membranes

The ionic conductivities (σ) of SPDA-IL and Nafion-IL membranes in anhydrous conditions were plotted as a function of temperature, see Fig. 8a. The corresponding conductivity increased exponentially with temperature from the order of 10^{-4} S cm^{-1} up to 10^{-2} S cm^{-1} at 160 °C. In general, the proton conductivity is strongly dependent on its nanostructure and water content. The decrease in the water content of the membrane results in low conductivity, due to not all of the acid sites being dissociated and a low level of interaction among water molecules, via hydrogen bonding. The conductivity of the IL-based membranes shows a similar trend to the water-based membrane. It may be due to the presence of IL resulting in an enhancement in the dissociation of protons from the sulfonated polymer causing an increase in proton transport mobility. The SPDA with a higher DS shows better ionic conductivity in the same range of temperatures (80–160 °C), which may be due to the larger number of sulfonic acid groups. In addition, the SPDA
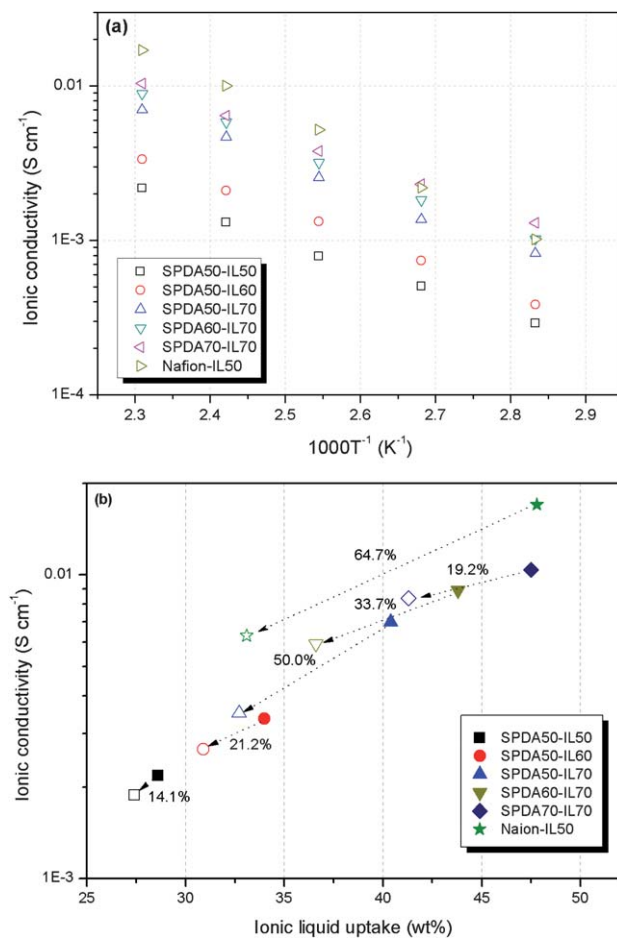

Fig. 8 Ionic conductivities as a function of temperature of SPDA-IL and Nafion-IL membranes in anhydrous conditions. (b) Ionic conductivity of the IL-uptake membranes before and after centrifugation.

with higher DS may provide better ion-conducting paths for proton conduction in the composite membrane. These results are consistent with previous results for membranes with different DS.[60–62]

Fig. 8b shows the ionic conductivities of the IL-uptake membranes before and after the centrifugal process. The Nafion-IL50 membrane shows a higher conductivity (1.7 mS cm^{-1}) compared to the SPDA-IL membranes at 160 °C, which is related to a longer flexible spacer (free volume) that facilitates the transportation of protons.[63,64] After centrifugation, the conductivities of all membranes decreased by more than the as-prepared ones (made without any centrifugation test), indicating a strong dependence on IL uptake in the membrane. In the case of a water-swelled electrolyte membrane, there are two main mechanisms for proton transport, namely proton hopping (Grotthuss mechanism) and diffusion (vehicular mechanism).[64] The two mechanisms may be adopted in this work as well. Before centrifugation, protons transport may occur by both hopping and diffusion in the membrane. However, after centrifugation, proton transport *via* diffusion is limited, since the amount of IL in the bulk phase that can facilitate proton diffusion is reduced. It is similar to proton transport under low humidity conditions for water-based electrolyte membranes. It is simply the case that after centrifugation, the SPDA membrane with a higher DS exhibits better proton transport, implying the presence of more sulfonic acid groups as well as a higher amount of IL in the membrane. In addition, the trend of variation in the proton conductivity is consistent with our supposition, *i.e.* that the conductivity reduction is less for membranes with higher DS.

For Nafion-IL composite membranes, a 64.7% reduction in its conductivity was observed after centrifugation (from 1.70 mS cm^{-1} to 0.63 mS cm^{-1}). In contrast, the conductivity of the SPDA70-IL70 membrane decreased from 1.04 mS cm^{-1} to 0.84 mS cm^{-1}, *i.e.* only a 19.2% in reduction. Although the Nafion-based composite membrane possesses a relatively higher conductivity than the sulfonated polymer, its proton conductivity significantly decreases after centrifugation, indicating the benefits of both a higher DS and the presence of a network structure in the membrane.

The H$_2$/O$_2$ fuel cell was operated at 100 °C using a SPDA50-IL70 and SPDA70-IL70 composite membrane without humidification (ESI†). The maximum power density was 98 mW cm^{-2} for the SPDA50-IL70 membrane and 122 for the SPDA70-IL70, which is approximately a 24% increase. This may be due to the higher DS of the SPDA70-IL70 increasing both the membrane IL retention and the proton conductivity. However, the performance is still much lower than that of conventional PEMFCs with hydrated ion exchange membranes. It is worth noting that the SPDA membrane was operated without humidification of the supplied gases (H$_2$ and O$_2$). Hence, this approach allows this type of IL-based cross-linked membrane to have potential applications in high-temperature polymer electrolyte membrane fuel cells.

Thermal stability of composite membranes

The thermal stabilities of pure IL (BMIm-BF$_4$), SPDA50, Nafion-IL50 and SPDA50-IL membranes were investigated by TGA as shown in Fig. 9. The corresponding onset temperatures
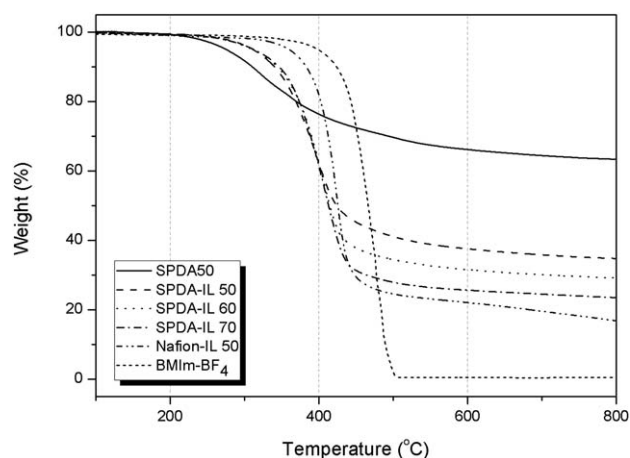

Fig. 9 TGA curves of pure IL (BMIm-BF$_4$), SPDA50, Nafion-IL50 and SPDA50-IL membranes.

for weight losses of 5% and 10% are listed in Table 2. The TGA curve of pure IL exhibits excellent thermal stability up to 400.5 °C, followed immediately by one-step decomposition. For cross-linked SPDA50 membranes, it shows a continuous weight loss between 225 °C and 520 °C, which is attributed to the decomposition of sulfonic acid groups and aliphatic segments of propargyl. However, the onset temperatures for 5 and 10 wt% weight losses are above 310 °C and 340 respectively, for all SPDA-IL membranes. It is evident that the decomposition by desulfonation of sulfonic acid groups has been suppressed and shifted to higher temperatures for all of the SPDA-IL membranes. It has been reported that the thermal stability of sulfonated polymers in the sodium form is much higher in comparison with that in acid form.[55,56] This observation confirms that the decomposition of sulfonic acid groups and aliphatic segments of propargyl is inhibited by the presence of IL since the protons originating from the sulfonic acid groups are partially replaced by the bulky cation of the IL, resulting in the increase of the thermal stability of the membrane.

Membranes employed in PEFCs operating in the range 100~200 °C, require a high degree of stability for long-term
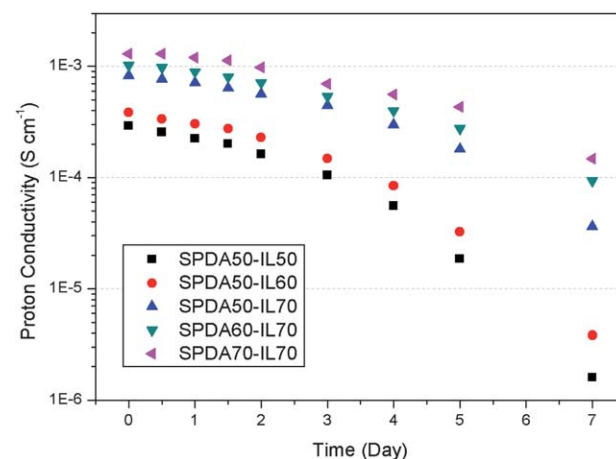

Fig. 10 Time-dependant proton conductivities of the SPDA-IL membranes under high temperature treatment (160 °C).

operation. The thermal stability of SPDA-IL membranes was also evaluated by thermal treatment for various times at 160 °C. Fig. 10 illustrates the time-dependant proton conductivities of the SPDA-IL membranes subjected to high temperature treatment (160 °C). Although the onset temperatures for 5 wt% weight loss for all the SPDA-IL membranes are similar (Table 2), the corresponding proton conductivity decays with a reduction of IL loading in the membrane. The result is basically inconsistent with the TGA study, where a higher IL content is able to improve the thermal stability of the membrane. Among these, the SPDA70-IL70 membrane with a higher IL loading maintains adequate proton conductivity ($>1 \times 10^{-4}$ S cm^{-1}) for one week (at 160 °C). This result, indicates that a higher DS results in a better distribution of IL domains in the membrane matrix and leads to an effective improvement in membrane stability.

Conclusions

A new type of sulfonated polymer, containing diacetylene groups in the main chain, was successfully synthesized via an oxidative coupling approach. FTIR, NMR and DSC were used to confirm the structures and the crosslinking behavior of the polymer and the IL-based membrane. After the introduction of a network structure and a high DS into the polymer matrix, the IL-based membranes exhibited a significant improvement in their thermal properties, dispersion of ionic domains, retention of IL and a reduction of proton conductivity loss. These IL-based membranes with higher amounts of IL and DS in the polymer matrix show higher ionic conductivities without humidification (ionic conductivity: SPDA50-IL50 = 0.21 mS cm^{-1}; SPDA70-IL70 = 1.02 mS cm^{-1}). As a comparison, the incorporation of a similar initial IL loading was found to reduce the proton conductivity loss of SPDA70-IL70 (19.2%) to about triple that of a IL-based Nafion membrane (64.6%), while showing a proton conductivity of more than 10^{-3} S cm^{-1} after centrifugation. In H$_2$/O$_2$ fuel cell operation using a composite membrane without humidification, a current density higher than 250 mA cm^{-2} was achieved with a maximum power denisty of 122 mW cm^{-2} at 100 °C. We believe this approach gives this type of IL-based cross-linked membrane potential applications in high-temperature polymer electrolyte membrane fuel cells.

Acknowledgements

References

1 T. Welton, Chem. Rev., 1999, 99, 2071.
2 Ionic Liquid: Industrial Applications for Green Chemistry; R. Rogers, K. Seddon, ed.; ACS Symposium Series 818; American Chemical Society: Washington, DC, 2002.
3 P. Wasserscheid and W. Keim, Angew. Chem., Int. Ed., 2000, 39, 3772.
4 R. D. Rogers and K. R. Seddon, Science, 2003, 302, 792–793.
5 J. Dupont, R. F. de Souza and P. A. Z. Suarez, Chem. Rev., 2002, 102, 3667.
6 M. A. Ratner and D. F. Shriver, Chem. Rev., 1988, 88, 109.
7 K. Xu, Chem. Rev., 2004, 104(10), 4303.
8 F. M. Gray, Polymer Electrolytes; RSC Materials Monographs; The Royal Society of Chemistry, Information Services: Letch-worth, U.K., 1997.
9 R. K. Ahluwalia and X. Wang, J. Power Sources, 2008, 177(1), 167.
10 G. Alberti, M. Casciola, L. Massinelli and B. Bauer, J. Membr. Sci., 2001, 185(1), 73.
11 Q. Li, R. He, J. O. Jensen and N. Bjerrum, Chem. Mater., 2003, 15, 4896.
12 K. -D. Kreuer, S. J. Paddison, E. Spohr and M. Schuster, Chem. Rev., 2004, 104, 4637.
13 M. S. Dresselhaus and I. L. Thomas, Nature, 2001, 414, 332.
14 J. Roziere and D. Jones, Annu. Rev. Mater. Res., 2003, 33, 503.
15 P. Wasserscheid, T. Welton, ed. Ionic Liquids in Synthesis; Wiley-VCH Verlag: Weinheim, Germany, 2003.
16 T. Ueki and M. Watanabe, Macromolecules, 2008, 41, 3739.
17 H. Chen, J. H. Choi, D. S. Cruz, K. I. Winey and Y. A. Elabd, Macromolecules, 2009, 42, 4809.
18 M. Susan, T. Kaneko, A. Noda and M. Watanabe, J. Am. Chem. Soc., 2005, 127(13), 4976.
19 S. Yu, F. Yan, X. Zhang, J. You, P. Wu, J. Lu, Q. Xu, X. Xia and G. Ma, Macromolecules, 2008, 41, 3389.
20 Feng Yan, S. Yu, X. Zhang, L. Qiu, F. Chu, J. You and J. Lu, Chem. Mater., 2009, 21, 1480–1484.
21 M. Doyle, S. K. Choi and G. Oroulx, J. Electrochem. Soc., 2000, 147, 34.
22 M. K. Mistry, S. Subianto, N. R. Choudhury and N. K. Dutta, Langmuir, 2009, 25(16), 9240.
23 R. H. Brown, A. J. Duncan, J. H. Choi, J. K. Park, T. Wu, D. J. Leo, K. I. Winey, R. B. Moore and T. E. Long, Macromolecules, 2010, 43(2), 790.
24 Y. Y. He and T. P. Lodge, Chem. Commun., 2007, 26, 2732.
25 Y. Y. He, P. G. Boswell, P. Buhlmann and T. P. Lodge, J. Phys. Chem. B, 2007, 111, 4645.
26 S. S. Sekhon, J. S. Park, E. Cho, Y. G. Yoon and C. S. Kim, Macromolecules, 2009, 42, 2054.
27 Q. Che, B. Sun and R. He, Electrochim. Acta, 2008, 53, 4428.
28 E. K. Cho, J. S. Park, S. S. Sekhon, G. G. Park, T. H. Yang, W. Y. Lee, C. S. Kim and S. B. Park, J. Electrochem. Soc., 2009, 156(2), B197.
29 S. Y. Lee, T. Yasuda and M. Watanabe, J. Power Sources, 2010, 195, 5909.
30 A. Fernicola, S. Panero and B. Scrosati, J. Power Sources, 2008, 178, 591.
31 J. Kim, S. Mulmi, C. Lee, H. Park, Y. Chung and Y. Lee, J. Membr. Sci., 2006, 283, 172.
32 F. Pereira, K. Vallé, P. Belleville, A. Morin, S. Lambert and C. Sanchez, Chem. Mater., 2008, 20, 1710.
33 Y. Jin, S. Qiao, L. Zhang, Z. Xu, S. Smart, J. Costa and G. Lu, J. Power Sources, 2008, 185, 664.
34 D. S. Phu, C. H. Lee, C. H. Park, S. Y. Lee and Y. M. Lee, Macromol. Rapid Commun., 2009, 30(1), 64.
35 J. Chen, M. Asano, Y. Maekawa and M. Yoshida, J. Polym. Sci., Part A: Polym. Chem., 2008, 46(16), 5559.
36 Y. S. Ye, Y. C. Yen, C. C. Cheng, W. Y. Chen, L. T. Tsai and F. C. Chang, Polymer, 2009, 50, 3196.
37 Y. S. Ye, W. Y. Cheng, Y. J. Huang, M. Y. Cheng, Y. C. Yen, C. C. Cheng and F. C. Chang, J. Membr. Sci., 2010, 362, 29.
38 Y. S. Ye, Y. J. Huang, C. C. Cheng and F. C. Chang, Chem. Commun., 2010, 46, 7554.
39 T. M. Miller, E. W. Kwock, T. Baird and A. Hale, Chem. Mater., 1994, 6(11), 1569.
40 Y. Qi and Z. Y. Wang, Macromolecules, 2003, 36, 3146.
41 Y. S. Ye, Y. C. Yen, C. C. Cheng, Y. S. Syu, Y. J. Huang and F. C. Chang, Polymer, 2010, 51, 430.
42 E. Cho, J. S. Park, S. S. Sekhon, G. G. Park, T. H. Yang, W. Y. Lee, C. S. Kim and S. B. Park, J. Electrochem. Soc., 2009, 156(2), B197.
43 M. Y. Cheng, C. J. Pan and B. J. Hwang, J. Mater. Chem., 2009, 19, 5193.
44 A. S. Hay, D. A. Bolon and K. R. Leimer, J. Polym. Sci., Part A-1, 1970, 8, 1022.
45 M.-F. Grenier-Loustalot, V. Denizot and D. Beziers, High Perform. Polym., 1995, 7, 157.
46 C. Badarau and Z. Y. Wang, Macromolecules, 2004, 37, 147.

47 A. Chernykh, T. Agag and H. Ishida, *Macromolecules*, 2009, **42**, 5121.
48 H. W. Beckham and T. M. Keller, *J. Mater. Chem.*, 2002, **12**, 3363.
49 Y. Xiaowu, Y. Luo, Y. Deng, Q. Yan, G. Zou and Q. Zhang, *Eur. Polym. J.*, 2008, **44**, 881.
50 K. M. Dieter, C. J. Dymek Jr, N. E. Heimer, J. W. Rovang and J. S. J. Wilkes, *J. Am. Chem. Soc.*, 1988, **110**, 2722.
51 N. Nanbu, Y. Sasaki and F. Kitamura, *Electrochem. Commun.*, 2003, **5**, 383.
52 S. K. Dirlikov and Y. Feng, *Poly. Prepr. (Am. Chem. Soc., Div. Polym. Chem.)*, 1991, **32**(1), 363.
53 L. G. Picklesimer, U.S. Patent 4, 2266, 800 (Oct 7, 1980).
54 H. Olivier-Bourbigou, *J. Mol. Catal. A: Chem.*, 2002, **182**, 419.
55 T. D. Gierke, G. E. Munn and F. C. Wilson, *J. Polym. Sci., Polym. Phys. Ed.*, 1981, **19**(11), 1687.
56 C. L. Marx, D. F. Caulfield and S. L. Cooper, *Macromolecules*, 1973, **6**, 344.
57 J. Kao, R. S. Stein, W. J. MacKnight, W. P. Taggart and G. S. Cargill, *Macromolecules*, 1974, **7**, 95.
58 W. J. MacKnight, W. P. Taggart and R. S. Stein, *J. Polym. Sci., Polym. Phys.*, 1974, **45**(1), 113.
59 R. H. Brown, A. J. Duncan, J. H. Choi, J. K. Oark, T. Wu, D. J. Leo, K. I. Winey, R. B. Moore and T. E. Long, *Macromolecules*, 2010, **43**(2), 790.
60 M. Doyle, S. K. Choi and G. Proulx, *J. Electrochem. Soc.*, 2000, **147**, 34.
61 Q. Che, B. Sun and R. He, *Electrochim. Acta*, 2008, **53**, 4428.
62 M. Yoshizawa and H. Ohno, *Electrochim. Acta*, 2001, **46**, 1723.
63 S. Washiro, M. Yoshizawa, H. Nakajima and H. Ohno, *Polymer*, 2004, **45**, 1577.
64 E. K. Cho, J. S. Park, S. S. Sekhon, G. G. Park, T. H. Yang, W. Y. Lee, C. S. Kim and S. B. Park, *J. Electrochem. Soc.*, 2009, **156**, B197.